Toxicology Research

PAPER

View Article Online
View Journal | View Issue

Cite this: *Toxicol. Res.*, 2018, **7**, 93

Systematic toxicity investigation of graphene oxide: evaluation of assay selection, cell type, exposure period and flake size†

V. Gies[a] and S. Zou *[a,b]

Received 17th October 2017,
Accepted 22nd November 2017

DOI: 10.1039/c7tx00278e

rsc.li/toxicology-research

Understanding the toxicity of nanomaterials is essential for the safe and sustainable development of new applications. This is particularly true for a nanomaterial as widely used as graphene oxide (GO), which is utilized as films for electronics, membranes for filtration, drug carriers and more. Despite this, the current literature presents conflicting results on the overall toxicity of GO. Here, the cytotoxicity of three sizes of commercially available GO was investigated on six cell lines, as values of NOAEL/LOAEL. The effectiveness of four viability assays was also evaluated. The overall toxicity of GO greatly varied between cell lines; the suspension cells showed a greater response to the GO treatment compared to the adherent cell lines. Time dependent cytotoxicity was also cell line dependent, with only one cell line demonstrating obvious dependence. The six cell lines were also tested to evaluate their response to varying GO flake sizes: the suspension/phagocytic cells showed little variation in viability, while a difference was observed for the adherent/non-phagocytic cell lines. By systematically studying the effect of dose, GO size and treatment time for the six cell lines by using commercially available GO samples, we eliminate many of the variables which may result in the conflicting reports on the cytotoxicity of GO in the literature.

Introduction

Graphene oxide (GO), a member of the 2-dimensional carbon family, is composed of sp^2-hybridized carbon atoms decorated with epoxides, alcohols, carboxylic acids and other keto groups.[2–4] Similar to graphene, GO demonstrates exceptional electronic, optical and mechanical properties but is inexpensive, easily produced in large quantities and versatile, providing a starting material for further functionalization.[1,3,5] The promising characteristics of GO have attracted much attention in the fields of materials science, physics, chemistry and biotechnology.[4] Transparent conductive films, solar cells, light emitting diodes and photodetectors have been produced to exploit the flexibility, optical transparency and electrical conductivity of GO and reduced-GO.[5,6] Recently, laminates of GO have been prepared for filtration and separation, benefitting from the internal low frictional water flow.[7] GO flakes were also used to adsorb dyes from waste water.[8,9] Moreover, GO is of particular interest in biological systems because of its hydrophilic nature;[10] this property allows for its use as carriers in drug delivery and probes in cellular imaging and biosensors.[11–15]

Due to the vast range of applications of GO, a thorough understanding of the cytotoxicity of GO is essential for the safe and sustainable development of GO based nanotechnologies.[16] *In vitro* toxicity measurements are a popular and effective starting tool to understand the cytotoxicity of materials. The toxicity of pristine GO has been an area of interest for many other groups.[10,17–23] Though toxicity is typically reported as the concentrations that result in the death of half of the cell population after 48 h exposure,[24] many current GO literature studies either did not reach 50% viability or did not study the 48 h exposure period. To facilitate comparisons, toxicity will be described with the no observed adverse effect level/lowest observed adverse effect level (NOAEL/LOAEL) where the NOAEL is the last concentration which results in a final viability higher than 80% and the LOAEL is the first concentration which results in a final viability lower than 80%. Common to most literature studies which evaluated the toxicity of GO, a dose dependent toxicity was observed where higher concentrations resulted in lower viabilities.[10,17–23,25] No consensus has been reached on the time dependence of the toxicity: both time dependent[18,23] and time independent[20,21] cytotoxicity of GO have been reported. Regarding the impact of size on the

[a]*Measurement Science and Standards, National Research Council Canada, 100 Sussex Drive, Ottawa, Ontario K1A 0R6, Canada. E-mail: shan.zou@nrc-cnrc.gc.ca*
[b]*Department of Chemistry, Carleton University, 1125 Colonel By Drive, Ottawa, Ontario K1S 5B6, Canada*

†Electronic supplementary information (ESI) available: Detailed material sources, sample preparation procedures, AFM, DLS and stability measurements. See DOI: 10.1039/c7tx00278e

toxicity, most results indicate that smaller flake sizes result in a greater toxicity;[19,20,23] however, one group studying comparatively low concentrations did not observe a size dependence on all cell lines studied.[10] The values reporting the overall toxicity of GO have also been largely inconsistent: the LOAEL was observed to be 10 μg mL^{-1} for HeLa cells,[22] two groups separately observed that 20–25 μg mL^{-1} GO was the LOAEL for A549 and skin fibroblast cells.[19,21] Another group which studied fibroblasts observed 50 μg mL^{-1} to be the LOAEL.[18] Finally, other literature studies suggest that GO is biocompatible and cells may even use GO as a surface to grow.[17,25] Some of the most commonly referenced studies which study the cytotoxicity of GO through proliferation/viability based assays are summarized in Table 1.

Many apparent contradictions are clearly present in the current literature evaluating the toxicity of GO on mammalian cells. There are large discrepancies among the overall toxicity and biocompatibility, the time dependence, the size and the type of assay used for GO toxicity measurements. In most of these studies, in-house prepared GO is usually studied only on one cell line using a single viability assay. It has been demonstrated that GO prepared through different methods (*e.g.* Hofmann, Staudenmaier, Tour and Hummers methods) has a different impact on the toxicity on human lung epithelium cells.[26] In-house prepared GO will likely vary in composition and purity between labs and further complicate the comparison of the results. Using the same source of GO will eliminate compositional and structural variances.

The viability assay and method used to calibrate the cytotoxicity may further influence the results. The two most common assays are the MTT assay and the WST-8 assay; both are based on the same principle. Briefly, a tetrazolium salt is reduced by metabolically active cells to produce a colored formazan and the measured optical density is then proportional to the number of metabolically active cells in the sample. Carbon nanotubes and other nanomaterials have been observed to interfere with the MTT assay[29,30] and Liao *et al.* even observed this to be the case for GO.[19] However, many other groups did not observe any interference.[21,22] Other assays used include the Alamar blue assay (another proliferation assay), trypan blue exclusion assay (a stain based assay), and the LIVE/DEAD assay (a fluorescence based assay).

In order to directly compare the data and understand the toxicity of GO, it is necessary to use a consistent source of GO with a systematic control on the size, dosage and time of treatment with different cell types while validating the effectiveness of the viability assay. We had recently developed a simple sonication and analysis approach to control and determine the size of GO flakes using commercially available materials.[31] In this work we applied this method to yield three different sizes of GO flakes and studied their cytotoxicity on six different cell lines: NIH 3T3, RAW 264.7, A549, U87, NB4 and HL60. Literature studies on a variety of nanomaterials have demonstrated that the cellular response is cell line dependent[32] which outlines the importance of studying multiple cell lines. Our selection of cells includes three adherent cell lines, one

Table 1 Summary of commonly referenced studies which used colorimetric, proliferation based assays to study the cytotoxicity of GO

Citation	Cell line	GO source	GO size (nm)	Assay used	Exposure period	Time effect?	Size effect?	LOAEL[a] (μg mL^{-1})
Chang[20]	A549	In house-modified Hummers method (In-HU)	*l*-GO: 750 ± 410 *m*-GO: 430 ± 300 *s*-GO: 160 ± 90	WST-8 & Trypan blue	24, 48, 72 h	No	Yes	*l*-GO: NT *m*-GO: NT *s*-GO: 200
Wang[18]	HDF	In-HU	Not-explored	WST-8	1–5 days	Yes	N/A	50
Hu[21]	A549	In-HU	Not explored	MTT	24, 12, 6, 4, 2 h	No	N/A	40
Liao[19]	CRL-2522	In-HU	pGO-30: 342 ± 17	MTT[b], WST-8 & TB stain	24 h	N/A	N/A	pGO-30: 25 μg mL^{-1}
Chng[26]	A549	In-house Hofmann (HO), Staudenmaier (ST), Tour (TO) and Hummers (HU)	N/A	MTT	24, 48 h	No	N/A	GO-ST: 8 GO-HO: 8 GO-HU: 2 GO-TO: NT
				WST-8		No	N/A	GO-ST: 8 GO-HO: 35 GO-HU: 8 GO-TO: 20
Das[23]	HUVEC	Cheap Tubes Inc.	S1: 400–800 S2: 200–800	MTT	24, 48 h	Yes	Yes	GOS1: 5 GOS2: 1
Yue[10]	PMØ, J774A1, MCF-7, Hep G2, LLC & HUVEC	In-HU	S1: 350 S2: 2000	WST-8	48 h	N/A	No	S1: 10[c] (HUVEC) S1 & S2: NT (other cells)
Zhang[22]	HeLa	In-HU	N/A	MTT	24 h	N/A	N/A	20
Peruzynska[27]	MCF7	In house	1000–15 000	WST-1	48 h	N/A	N/A	100[c]
Contreras-Torres[28]	H9c2	In-TO	380	Alamar blue	24 h	N/A	N/A	100

[a] Concentrations listed represent the lowest observed adverse effect level, the first concentration that resulted in a final viability lower than 80% after 24 h exposure. Non-toxic (NT) is listed if less than 80% viability was not reached for the concentrations studied. [b] GO was observed to interfere with the MTT assay and the assay was deemed unsuitable for GO toxicity evaluation. [c] After 48 h exposure.

semi-adherent cell line and two suspension cell lines and within this selection one is phagocytic and five non-phagocytic cells. Brain, lung, blood and structural tissues are all represented in this selection and demonstrate how GO may affect different target areas within the body. To accomplish this, we first studied four viability assays to explore which assay yields the most reliable results and is most appropriate for studying the cytotoxicity of GO. No fluorescence based assays were selected as it has been demonstrated that they may not be suitable for the quantification of the toxicity of carbon nanomaterials due to fluorescence quenching.[33,34]

Methods

Materials

Graphene oxide, 4 mg mL^{-1}, was purchased from Graphenea (Gipuzkoa, Spain) and diluted to 2 mg mL^{-1} with sterile water as the stock solution for further dilutions. All other materials and cell culture media information can be found in the ESI.†

Graphene oxide sample preparation

2 mg mL^{-1} Graphenea GO was sonicated at 4 °C until a set amount of energy was delivered to the sample. Table S1† reports the sonication times and energies used to produce three distinct sizes of GO.

Dynamic light scattering (DLS) measurements

DLS measurements of GO samples of varying sizes were performed on the Zetasizer Nano ZS particle size analyser (Malvern Instruments, Worc, UK) in a semi-micro polystyrene disposable cuvette (VWR, PA, USA). Samples for DLS were diluted to 2 μg mL^{-1} in MilliQ water. Measurements were performed at 25 °C with 180 s of equilibration time. More details are included in the ESI.†

Atomic force microscopy (AFM) measurements

AFM height/topography images were recorded using a MultiMode NanoScope V with PeakForce QNM (Bruker Nano Surfaces Division, Santa Barbara, CA, USA). ScanAsyst-Air probes with a typical spring constant of 0.4 N m^{-1} and a resonance frequency of 50–90 kHz were used. The peak force was always maintained at the lowest stable imaging level of 200–500 pN. Details regarding samples, imaging parameters and data processing are included in the ESI.†

Cell viabilities

For the three formazan based assays, cells were seeded in a 96 well, flat bottom plate and treated with 5, 10, 20, 30, 50, 75, 100 and 200 μg mL^{-1} of GO for a predetermined exposure period of either 24, 48 or 96 h. Following the exposure period, the assay reagent was added for the MTS and WST-8 assays. Additional treatment details for the MTT assay and control experiments for all assay tests can be found in the ESI.†

Bright field imaging

Cells were seeded in a 24 well, flat bottom plate and treated with the same series of GO concentrations. After the exposure period, the cells were washed twice with PBS and images were recorded on the Olympus LX81-DSU Microscope (Olympus America Inc., NY, USA) using the CoolSNAP ES Camera (Photometrics, AZ, USA) and X-Cite Series 12OPC excitation source (Excelitas Technologies, QC, Canada) with a 20× objective (Olympus America INC, NY, USA). Exposure period, detailed cell treatment and conditions are outlined in the ESI.†

Results and discussion

GO size control and evaluation

The size of GO, as with many nanomaterials, impacts the materials' characteristics and properties.[35] Moreover, size tailored GO flakes are needed to meet a broad range of applications. We have recently developed a new method to manipulate the size of GO flakes *via* probe sonication and quantify the resulting flake size through DLS and AFM.[31] Detailed changes in the GO flake size (30 different sized samples) controlled by sonication energies are included in Fig. S1.† Here, we modified and applied this new method to control the GO flake size and selected three distinct sizes of GO for further tests: 150 nm small GO (*s*-GO); 250 nm medium GO (*m*-GO) and 1000 nm large GO (*l*-GO). See Table S1† for the sonication time and energies which led to these flake sizes.

The three flake sizes were characterized by both DLS and AFM. It should be noted that the intensity-weighted equivalent sphere hydrodynamic diameter is determined by the DLS measurements, while in AFM, the number-weighted average Feret's diameter is measured. Table 2 summarizes the average flake sizes of the three GO samples determined through these two methods.

Fig. 1 also demonstrates the width of the flake size distributions of the three samples by both AFM and DLS. The width is the smallest for *s*-GO and the largest for *l*-GO. This is likely because less energy is required to break apart the large flakes compared to the small flakes and they are therefore first to degrade. From DLS and AFM, we were able to measure and confirm the flake size of the three sets of samples. These three samples were then used to understand the size dependent toxicity of GO.

From the AFM height images shown in Fig. 1, it can be seen that the flakes are smooth, do not contain holes or

Table 2 Average sizes of GO flakes determined by DLS and AFM

GO sample	Hydrodynamic diameter determined by DLS (nm)	Feret's diameter determined by AFM (nm)
s-GO	154 ± 6	151 ± 7
m-GO	240 ± 14	233 ± 10
l-GO	1040 ± 47	974 ± 29

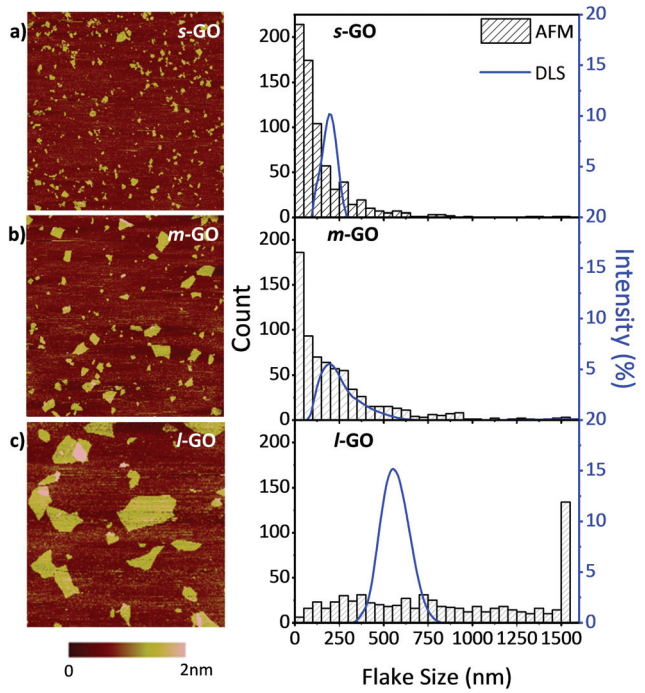

Fig. 1 AFM height images and histograms of the GO flake diameters of (a) *s*-GO, (b) *m*-GO and (c) *l*-GO. The histograms determined by AFM are overlaid with size distributions measured by DLS (blue lines, right axis).

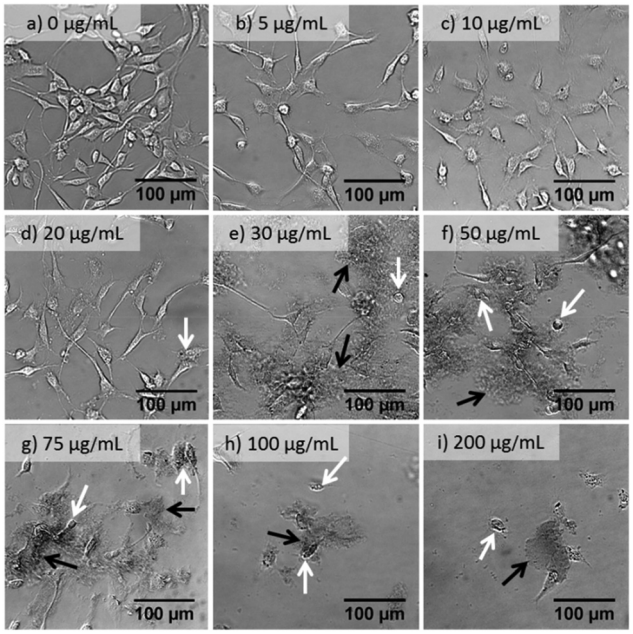

Fig. 2 Bright field images of NIH 3T3 cells after 24 h of exposure to a series of concentrations of GO after two PBS washings. The value listed on the image is the concentration of *s*-GO. White arrows indicate cell blebbing and/or shrunken cells. Black arrows point to the retained GO, which is darker in color.

defects and are mostly uniform in height, which indicates that sonication does not introduce obvious damage to the GO flakes. It was observed that the average GO flake size can be reliably tuned *via* a range of controlled sonication energies.

Configurational changes and cellular interactions with GO

Bright field imaging allows, and is often used for, the observation of configurational changes in cell morphology upon nanomaterial treatments.[18,36,37] These morphology changes may provide information regarding the cellular interactions with external factors, illustrate cell growth or death based on confluency and population *vs.* a control in response to an external factor.[37] An initial measurement of cytotoxicity of GO may be assessed through bright field imaging.

Fig. 2 shows bright field images of NIH 3T3 cells after 24 h exposure to a series of concentrations of *s*-GO. NIH 3T3 cells were selected for imaging due to their distinct morphology which facilitates the visual evaluation of the cell health. As the concentration of *s*-GO increased from 5 to 50 μg mL^{-1}, the images have increased amounts of dark, non-cellular features, which then decreased as the concentration increased to 200 μg mL^{-1}. These features were recognized as *s*-GO flakes and aggregates, which were not washed away after two PBS rinses. It cannot be clearly determined if the *s*-GO was under, inside or attached to the outside of the cell. GO has been observed to act as a surface for cellular growth.[17,25] Although the 150 nm surface is likely too small for the cells to use to grow, they may still be attaching to the flakes and retaining the material. This could provide an explanation for the initial increase of retained GO followed by a decrease; only viable cells would be able to retain the GO and would therefore be washed away at high concentrations where few viable cells remain.

At low concentrations (5 and 10 μg mL^{-1} of *s*-GO) few configurational changes were observed: the cells remained adherent with intercellular networks, though they appeared to be less populous. At 20 μg mL^{-1}, the cells began to show configurational signs of apoptosis, a few cells have shrunk, and some show blebbing (white arrow in Fig. 2d) and less cellular networking. At concentrations of 30 μg mL^{-1} and higher, increased amounts of cell shrinkage and blebbing are shown until few viable cells were present (Fig. 2e–i).

Imaging of NIH 3T3 cells treated with varying amounts of GO allowed for the initial, qualitative evaluation of GO's cytotoxic effects. Quantifying the cytotoxicity of GO through bright field imaging is, however, not feasible. To quantify the cytotoxicity of GO we performed various viability assays.

Proliferation assay evaluation

Cell based assays are a popular and effective tool for screening the effect of materials on a cell population.[38] Ensuring that the assay chosen gives reproducible and accurate results is crucial to obtain meaningful information on the cytotoxicity of the material studied[39] and may produce more relevant *in vivo* predictions.[40] Before beginning to study the cytotoxicity of GO on a variety of cell lines, we first demonstrated that none of the formazan based assays' reagents were reduced by the GO flakes to produce falsely high viabilities (see Fig. S3†). We then explored the reproducibility and compared the results of four

different viability assays on the NIH 3T3 cells using *s*-GO. The results are displayed in Fig. 3.

For the 24 h exposure period, the NOAEL/LOAEL values were determined to be 5/10, 10/20, 20/30 and 10/20 μg mL^{-1} for the TB stain, WST-8, MTS and MTT assays, respectively. These values did not greatly change for the 48 h exposure period. The NOAEL/LOAEL was 0/5 μg mL^{-1} for the TB stain, WST-8 and MTS assays, and 5/10 μg mL^{-1} for the MTT assay after 96 h exposure.

To understand which assays agreed well with one another, and are likely the most valid, the entire toxicity profile must be analysed. The TB stain, WST-8 and MTT assays indicate that there is a concentration dependent toxicity in which the viability of the cells gradually decreases along the concentrations studied. The TB stain and WST-8 assay results are in very close agreement with one another, both assays show less than 10% viable cells for GO concentrations higher than 100 μg mL^{-1} and show a similar change in viability as a response to concentration. The MTS assay resulted in values similar to the TB stain and WST-8 assay for the 48 and 96 h exposure periods as well as the 24 h exposure period for low concentrations. Deviations between the MTS assay and the TB stain/WST-8 assays began to occur for the higher concentrations, and the viabilities determined from the MTS assay were higher. Equating precision of measurements to reliability, the WST-8 assay is the most reliable assay, yielding the smallest standard error.

The MTT assay results were not in agreement with the trends observed in the other three assays. All other assays showed a gradual decrease in viability while the MTT assay showed a plateau followed by a fast drop in viability for the 24 h period and a sharp decrease, increase and decrease in viability were observed for the 48 and 96 h periods. This bizarre trend was attributed to the cells retaining the GO as observed in Fig. 3 (particularly in Fig. 3F). The MTT assay requires the cells to be washed before the addition of the assay reagent which is in part used to remove any of the material under investigation so that the material does not impact the absorption measurements. Since the GO was retained by viable cells and not washed away, the retained GO likely impacted the absorption measurements. The greatest impact was observed at moderate concentrations which is consistent with this theory; there was enough GO to impact the absorption measurements combined with enough viable cells (~30%, as determined by the other assays) to retain the GO. Despite MTT being one of the most commonly used cytotoxicity assays due to its high sensitivity and low cost, this phenomenon combined with the possible reactivity of GO with MTT observed in other studies[19] suggests that MTT is not an ideal assay to study the cytotoxicity of GO.

The assay which was favoured overall was the WST-8 assay. This assay resulted in the most reproducible and meaningful results and did not require intensive sample preparation. Furthermore, the WST-8 assay is commonly used in other studies which facilitates comparison. The WST-8 assay was selected to perform all other cytotoxicity measurements.

Cell line dependent cytotoxicity of GO

The cytotoxicity of *s*-GO was studied on six different cell lines using the WST-8 assay. The LOAEL values, the concentrations that resulted in a final viability lower than 80%, are summarized in Fig. 4. It is worth noting that the dispersion stability of GO is greatly reduced in cell culture media compared to water and is relatively low at high concentrations. It was observed

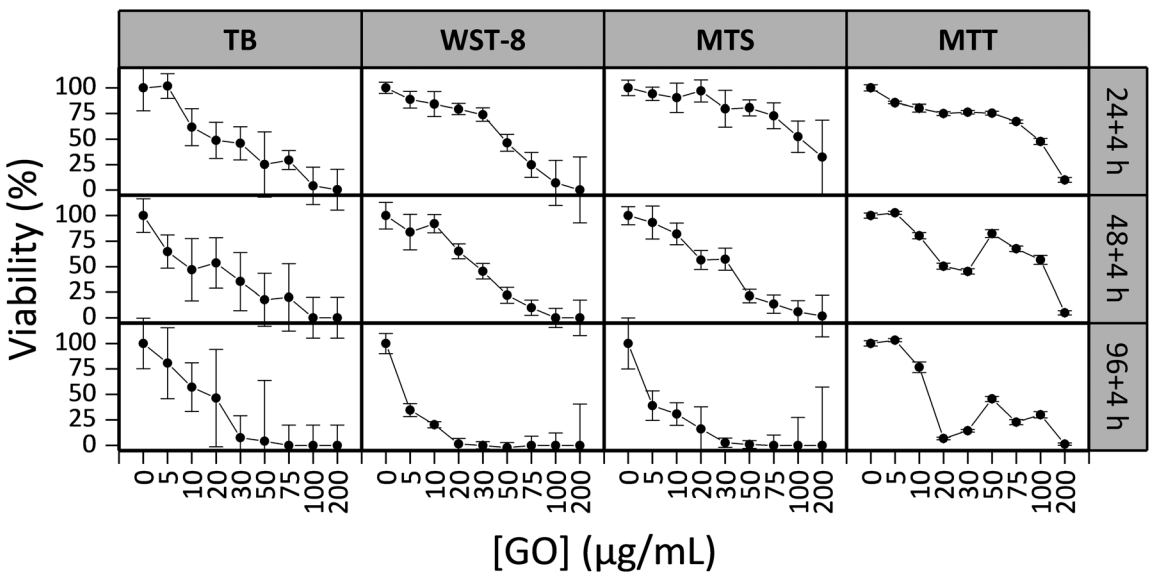

Fig. 3 Viability profiles of the NIH 3T3 cells after exposure to a series of concentrations of GO determined by four different colorimetric assays: TB stain, WST-8, MTS and MTT for 24, 48 and 96 h (plus 4 h incubation with the assay reagent). The TB stain assay represents two trials of two replicates. For the WST-8, MTS and MTT assays: up to six wells were recorded for each concentration in a given trial and a minimum of 2 trials were performed. Error bars represent the standard errors of the corresponding measurements.

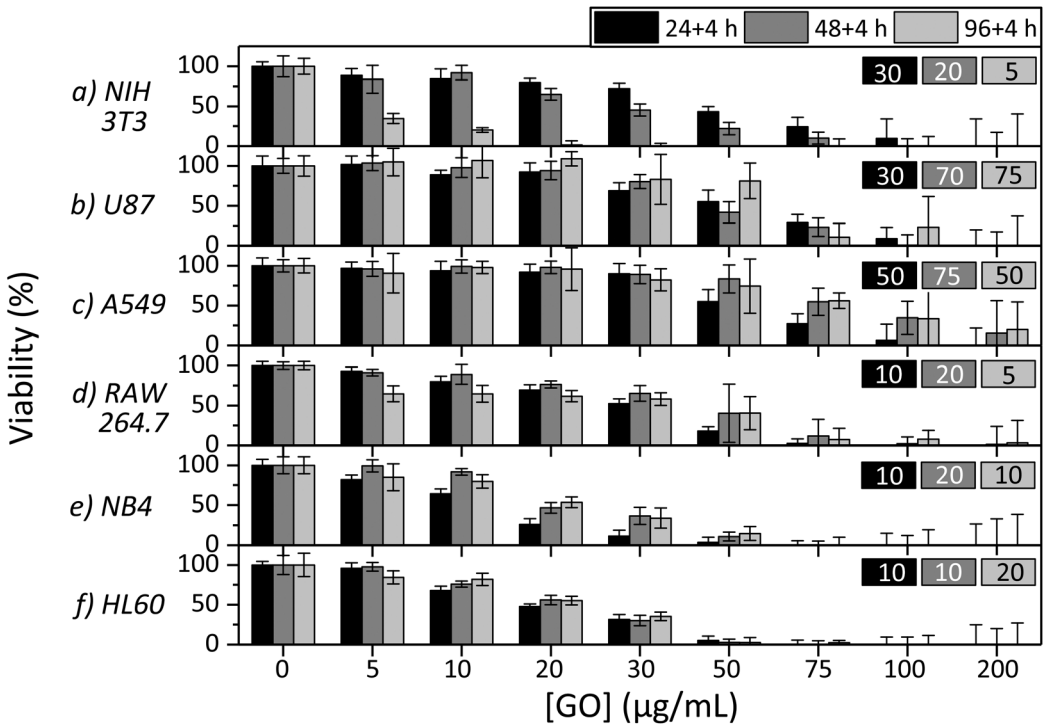

Fig. 4 Percent viability after treatment with varying concentrations of *s*-GO for (a) NIH 3T3, (b) U87, (c) A549, (d) RAW 264.7, (e) NB4 and (f) HL60 cells using the WST-8 assay for 24, 48 and 96 h (plus 4 h incubation with the assay reagent) exposure times. At least two trials of six replicates were performed for each cell line at each concentration at each time. Error bars represent the standard error of the measurements. Values at the upper right corner of each panel represent the LOAEL (the concentration that resulted in <80% viability) for their respective cell lines for 24, 48 and 96 h exposure periods.

that obvious instability began to occur at 75 μg mL^{-1} and was most evident at the highest concentration, 200 μg mL^{-1}. To further investigate the dispersion stability of GO, transmission measurements were performed on *s*-GO and *l*-GO at 50 μg mL^{-1} and *s*-GO at 200 μg mL^{-1}. The transmission of the samples and the images of the samples at 0 h and 24 h post mixing are shown in Fig. S2.† Briefly, 50 μg mL^{-1} *s*-GO and *l*-GO were observed to be stable, the change in transmission of the samples over 24 h was 20% and 15%, respectively, and no settled material was observed. 200 μg mL^{-1} *s*-GO had low stability, the transmission changed by 45% and a significant material was observed to settle. The stability and dispersability of nanomaterials certainly impacts the observed toxicity.[41] Low dispersability may result in a lower observed toxicity due to reduced material–cellular interactions, depending on the route of toxicity. Furthermore, when measuring the viability of cells with colorimetric assays, settled GO aggregates likely influence the absorption and scattering by causing inconsistent changes in the optical density of the samples. This may result in larger errors in the final results, which is observed with increasing GO concentrations in Fig. 4. Interestingly, the concentrations where this impact is the greatest are generally above the concentrations which result in the obvious toxicity for all cell lines.

In Fig. 4, the NOAEL/LOAEL values for the NIH 3T3 cell line were observed to be 20/30, 10/20 and 0/5 μg mL^{-1} of *s*-GO for 24, 48 and 96 h post exposure, respectively. Of the cell lines studied, the NIH 3T3 cell line was the only one to demonstrate a time dependence on the toxicity, and the U87 cell line was even observed to recover after 96 h with the NOAEL/LOAEL values being 20/30, 30/50, and 50/75 μg mL^{-1} of *s*-GO for 24, 48 and 96 h post exposure, respectively. The remaining four cell lines, A549, RAW 264.7, NB4 and HL60, did not demonstrate much variation in response to exposure time and the NOAEL/LOAEL values were 30/50, 5/10–10/20, 5/10 and 5/10 μg mL^{-1} GO, respectively. The change in proliferation as a response to increasing concentrations of GO is gradual and reasonably steady for all of the cell lines studied.

It is clear that the NOAEL/LOAEL values are not universal, even when using the same source of GO, and depends on the cell line. Cell line dependent toxicity has been previously observed for other nanomaterials.[32] More interestingly, a trend which relates the cell type to toxicity was observed. Relatively, the adherent cell lines, NIH 3T3, U87 and A549, showed the least change in proliferation as a response to GO, the semi-adherent cell line, RAW 264.7, showed moderate change, while the suspension cell lines (white blood cells), NB4 and HL 60, showed the greatest response. This indicates that GO is the least toxic on the adherent cell lines and the most toxic on the suspension cell lines. This observation could provide information on the route of toxicity of GO as Akhavan *et al.* showed that reduced GO was more toxic than GO on bacteria.[42] They

attributed this to the sharper nanowalls of the reduced GO. Our work provides evidence to support this theory for mammalian cells. The suspension cells are entirely exposed to the GO dispersion in three dimensions and thus increase the probability of cell–GO interactions, when only a portion of the adherent cells' surfaces are exposed to GO. As a result, the suspension cells have more contacts with the sharp edges of GO and potentially have increased cell damage resulting in death. The time dependence of the toxicity of GO is also important for understanding the origin of the toxicity and has been of interest to other groups. Hu *et al.* and Chang *et al.* observed no time dependence for the A549 cell line. Other studies on fibroblasts did observe a dependence on exposure period.[18–21] Here we have demonstrated that the conflicting results were not the outcome of a different experimental set up but that the time dependence on the toxicity is more likely cell line dependent.

To investigate whether the toxicity observed in this work was due to GO or due to contamination introduced into the sample during processing, experiments with control samples were performed. Sterile water was processed identical to *s*-GO and used to treat both the NIH 3T3 and the NB4 cell lines. The resulting viability of the cells (>98% viability) indicated that processing did not impact the apparent toxicity of GO.

Manganese, commonly used in the synthesis of GO *via* the Hummers method, is known to impact the toxicity of GO.[10] To explore if manganese or other toxic metal ions may be present in the sample, additional control experiments were performed which exploited the comparatively low stability of GO to the stability of metal ions in water. Centrifugation was used to extract the suspending water (supernatant) from the GO samples of both *s*-GO and the as received GO. The toxicity of the suspending water was evaluated on the NIH 3T3 and the NB4 cell lines. Both the as received and the *s*-GO samples demonstrated similar toxicity. The viability was reduced to 88 ± 6% for the NIH 3T3 cells and 71 ± 6% for NB4. It is not surprising that the NB4 cells showed a greater response than the NIH 3T3 cells as they also had a greater response to the complete GO samples. The toxicity of the suspending water may be a result of metal ions present in the Graphenea GO sample, from small, highly soluble flakes of GO (*i.e.*, oxidized debris form of GO), or simply because the pH value (pH ~ 3) of the suspending water was lower than ideal conditions for cell growth. Despite the impact on toxicity due to factors which are not the bulk GO flakes, the impact on the toxicity would be evenly affected for all samples studied under the same experimental conditions using the same source of GO.

GO size dependent cytotoxicity

Three sizes of GO, *s*-GO, *m*-GO and *l*-GO were studied using NIH 3T3, U87, A549, RAW 264.7, NB4 and HL60 cells. The size range of 150–1000 nm was chosen because it covers most of the range of the possible sizes of commercially available GO samples such as Graphenea GO. A more detailed explanation of the flake size selection is found in the ESI.†

A flake size dependence on the cytotoxicity of GO is observed for NIH 3T3, U87 and A549 cells, as shown in Fig. 5. In general,

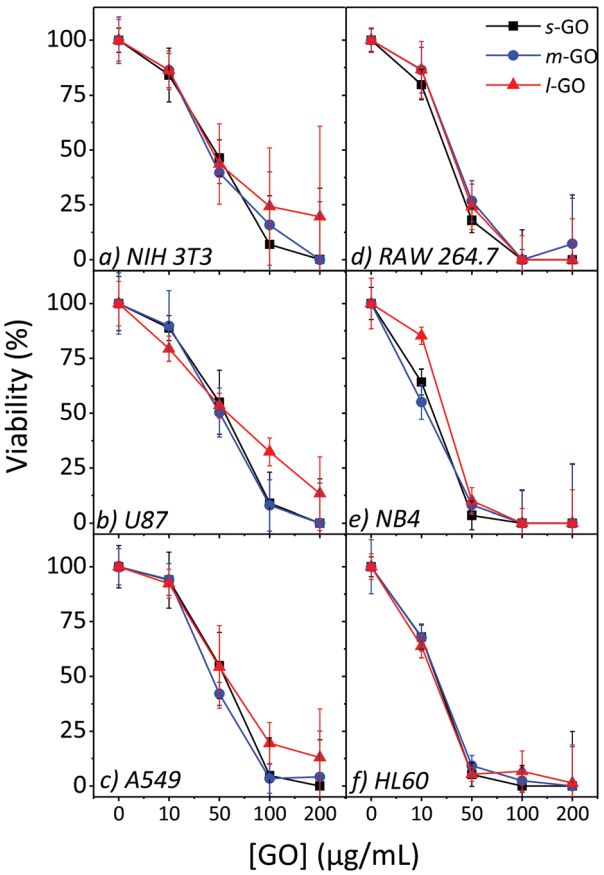

Fig. 5 Cytotoxicity profiles of *s*-GO, *m*-GO and *l*-GO on NIH 3T3, A549 and RAW 264.7 cells using the WST-8 assay after 24 h (plus 4 h incubation with the assay reagent) of exposure.

the largest flake size has lower cytotoxicity while smaller sized GO displays higher toxicity and lower cell viabilities. At the highest concentration studied, 200 μg mL^{-1}, *s*-GO and *m*-GO resulted in no or very few viable cells, but up to 20% of cells remained viable when exposed to *l*-GO. The difference in toxicity as a response to size increases with increasing concentrations; all three sizes have a similar toxicity at 10 μg mL^{-1} but, at 100 μg mL^{-1} the difference in toxicity as a response to flake size becomes obvious. The difference in toxicity between *s*-GO and *m*-GO is much less than the difference in toxicity between *s*-GO and *l*-GO, likely since *s*-GO and *m*-GO are closer in size than *s*-GO and *l*-GO. There was little impact on toxicity as a response to size for the RAW 264.7, NB4 and HL60 cell lines.

Several papers in the literature have studied the relationship between size and cytotoxicity and have reported a size dependence effect.[19,20,23] The smaller GO flakes may become internalized by the cells more readily resulting in higher toxicity, though a consensus regarding the cellular uptake of GO has not been reached.[18,20,22] Sharp edges of GO were observed to result in bacteria inactivation;[42] the smaller flakes have more available edges and may account for the difference in toxicity. Further evidence has been brought forward to suggest that the structure of GO may impact the cytotoxicity. In studies

evaluating the oxygen content and the presence of oxygen containing functional groups, the results have indicated that a lower C : O ratio may result in a higher toxicity.[23]

The RAW 264.7, NB4 and HL60 cell lines on the other hand did not follow this trend. This difference may be due to the nature of the cell. Studies which report that the flake size impacts the toxicity frequently study non-phagocytes, adherent cells like fibroblasts or epithelial cells. The work of Yue *et al.* studied both phagocytes and non-phagocytic cells and observed that there is not always a dependence on the size, and no dependence on the size was observed for the two phagocytic cell lines studied.[10] Here, higher concentrations were tested and provided further results to support that the toxicity of GO on phagocytes is not flake size dependent and adds evidence to suggest that this is also true for non-phagocytic suspension cells.

Conclusion

The impact of cell type, exposure period and flake size on the cytotoxicity of GO was systematically evaluated using the same source of the commercially available GO with precise processing controls. To accomplish this, four viability assays were considered: TB stain, MTT, MTS and WST-8. The WST-8 assay was determined to yield the most reproducible results and was chosen to perform the remaining studies. The cytotoxicity of GO was observed to vary between cell lines and more importantly, cell line types. GO had the least impact on the viability of adherent cells, and the NOAEL/LOAEL was observed to be between 10/20 and 20/30 μg mL^{-1}. GO had a greater impact on the semi-adherent cell line with the observed NOAEL/LOAEL being 10/20 μg mL^{-1} and GO had the greatest impact on the suspension cells where 5/10 μg mL^{-1} was observed to be the NOAEL/LOAEL (24 h post exposure). Time dependence on the cytotoxicity of GO was observed only for the NIH 3T3 cell line, the remaining cells showed little variance as a result of exposure period. The cytotoxicity of three sizes of GO was studied and a relationship between the size and cytotoxicity was observed for the three adherent cell lines: NIH 3T3, A459 and U87. No size dependence was observed for the semi-adherent and suspension cells: RAW 264.7, NB4 and HL60. This observation may be attributed to the difference between phagocytes and non-phagocytic cells and/or suspension *vs.* adherent cells.

Conflicts of interest

There are no conflicts of interest to declare.

Acknowledgements

The authors acknowledge the technical assistance of Drs Zhengfang Lu, Mahyar Mazluumi and Zygmunt Jakubek on the optical imaging and stability tests.

This work was supported by the National Research Council Canada under the Measurement Science for Emerging Technology Program.

References

1 Z. Guo, S. Wang, G. Wang, Z. Niu, J. Yang and W. Wu, Effect of oxidation debris on spectroscopic and macroscopic properties of graphene oxide, *Carbon*, 2014, **76**, 203–211.
2 M. Acik, G. Lee, C. Mattevi, M. Chhowalla, K. Cho and Y. Chabal, Unusual infrared-absorption mechanism in thermally reduced graphene oxide, *Nat. Mater.*, 2010, **9**, 840–845.
3 J. P. Rourke, P. A. Pandey, J. J. Moore, M. Bates, I. A. Kinloch, R. J. Young and N. R. Wilson, The real graphene oxide revealed: Stripping the oxidative debris from the graphene-like sheets, *Angew. Chem., Int. Ed.*, 2011, **50**, 3173–3177.
4 H. Y. Mao, S. Laurent, W. Chen, O. Akhavan, M. Imani, A. A. Ashkarran and M. Mahmoudi, Graphene: Promises, facts, opportunities, and challenges in nanomedicine, *Chem. Rev.*, 2013, **113**, 3407–3424.
5 Y. Zhu, S. Murali, W. Cai, X. Li, J. W. Suk, J. R. Potts and R. S. Ruoff, Graphene and graphene oxide: Synthesis, properties, and applications, *Adv. Mater.*, 2010, **22**, 3906–3924.
6 F. Bonaccorso, Z. Sun, T. Hasan and A. Ferrari, Graphene photonics and optoelectronics, *Nat. Photonics*, 2010, **4**, 611–622.
7 R. Joshi, P. Carbone, F.-C. Wang, V. G. Kravets, Y. Su, I. V. Grigorieva, H. Wu, A. K. Geim and R. R. Nair, Precise and ultrafast molecular sieving through graphene oxide membranes, *Science*, 2014, **343**, 752–754.
8 S.-T. Yang, S. Chen, Y. Chang, A. Cao, Y. Liu and H. Wang, Removal of methylene blue from aqueous solution by graphene oxide, *J. Colloid Interface Sci.*, 2011, **359**, 24–29.
9 Y. Li, Q. Du, T. Liu, J. Sun, Y. Wang, S. Wu, Z. Wang, Y. Xia and L. Xia, Methylene blue adsorption on graphene oxide/calcium alginate composites, *Carbohydr. Polym.*, 2013, **95**, 501–507.
10 H. Yue, W. Wei, Z. Yue, B. Wang, N. Luo, Y. Gao, D. Ma, G. Ma and Z. Su, The role of the lateral dimension of graphene oxide in the regulation of cellular responses, *Biomaterials*, 2012, **33**, 4013–4021.
11 X. Sun, Z. Liu, K. Welsher, J. T. Robinson, A. Goodwin, S. Zaric and H. Dai, Nano-graphene oxide for cellular imaging and drug delivery, *Nano Res.*, 2008, **1**, 203–212.
12 J. Liu, L. Cui and D. Losic, Graphene and graphene oxide as new nanocarriers for drug delivery applications, *Acta Biomater.*, 2013, **9**, 9243–9257.
13 S. Goenka, V. Sant and S. Sant, Graphene-based nanomaterials for drug delivery and tissue engineering, *J. Controlled Release*, 2014, **173**, 75–88.

14 Z. Liu, B. Liu, J. Ding and J. Liu, Fluorescent sensors using DNA-functionalized graphene oxide, *Anal. Bioanal. Chem.*, 2014, **406**, 6885–6902.
15 F. Wang and J. Liu, Platinated DNA oligonucleotides: New probes forming ultrastable conjugates with graphene oxide, *Nanoscale*, 2014, **6**, 7079–7084.
16 A. B. Seabra, A. J. Paula, R. de Lima, O. L. Alves and N. Durán, Nanotoxicity of graphene and graphene oxide, *Chem. Res. Toxicol.*, 2014, **27**, 159–168.
17 S.-R. Ryoo, Y.-K. Kim, M.-H. Kim and D.-H. Min, Behaviors of NIH-3T3 fibroblasts on graphene/carbon nanotubes: Proliferation, focal adhesion, and gene transfection studies, *ACS Nano*, 2010, **4**, 6587–6598.
18 K. Wang, J. Ruan, H. Song, J. Zhang, Y. Wo, S. Guo and D. Cui, Biocompatibility of graphene oxide, *Nanoscale Res. Lett.*, 2010, **6**, 8.
19 K.-H. Liao, Y.-S. Lin, C. W. Macosko and C. L. Haynes, Cytotoxicity of graphene oxide and graphene in human erythrocytes and skin fibroblasts, *ACS Appl. Mater. Interfaces*, 2011, **3**, 2607–2615.
20 Y. Chang, S.-T. Yang, J.-H. Liu, E. Dong, Y. Wang, A. Cao, Y. Liu and H. Wang, In vitro toxicity evaluation of graphene oxide on A549 cells, *Toxicol. Lett.*, 2011, **200**, 201–210.
21 W. Hu, C. Peng, M. Lv, X. Li, Y. Zhang, N. Chen, C. Fan and Q. Huang, Protein corona-mediated mitigation of cytotoxicity of graphene oxide, *ACS Nano*, 2011, **5**, 3693–3700.
22 X. Zhang, W. Hu, J. Li, L. Tao and Y. Wei, A comparative study of cellular uptake and cytotoxicity of multi-walled carbon nanotubes, graphene oxide, and nanodiamond, *Toxicol. Res.*, 2012, **1**, 62–68.
23 S. Das, S. Singh, V. Singh, D. Joung, J. M. Dowding, D. Reid, J. Anderson, L. Zhai, S. I. Khondaker and W. T. Self, Oxygenated functional group density on graphene oxide: Its effect on cell toxicity, *Part. Part. Syst. Charact.*, 2013, **30**, 148–157.
24 A. K. Jain, N. Kumar Mehra, N. Lodhi, V. Dubey, D. K. Mishra, P. K. Jain and N. K. Jain, Carbon nanotubes and their toxicity, *Nanotoxicology*, 2007, **1**, 167–197.
25 O. N. Ruiz, K. S. Fernando, B. Wang, N. A. Brown, P. G. Luo, N. D. McNamara, M. Vangsness, Y.-P. Sun and C. E. Bunker, Graphene oxide: A nonspecific enhancer of cellular growth, *ACS Nano*, 2011, **5**, 8100–8107.
26 E. L. K. Chng and M. Pumera, The toxicity of graphene oxides: Dependence on the oxidative methods used, *Chem. – Eur. J.*, 2013, **19**, 8227–8235.
27 M. Peruzynska, K. Cendrowski, M. Barylak, M. Tkacz, K. Piotrowska, M. Kurzawski, E. Mijowska and M. Drozdzik, Comparative in vitro study of single and four layer graphene oxide nanoflakes—Cytotoxicity and cellular uptake, *Toxicol. in Vitro*, 2017, **41**, 205–213.
28 F. F. Contreras-Torres, A. Rodríguez-Galván, C. E. Guerrero-Beltrán, E. Martínez-Lorán, E. Vázquez-Garza, N. Ornelas-Soto and G. García-Rivas, Differential cytotoxicity and internalization of graphene family nanomaterials in myocardial cells, *Mater. Sci. Eng., C*, 2017, **73**, 633–642.
29 G. Ciofani, S. Danti, D. D'Alessandro, S. Moscato and A. Menciassi, Assessing cytotoxicity of boron nitride nanotubes: Interference with the MTT assay, *Biochem. Biophys. Res. Commun.*, 2010, **394**, 405–411.
30 L. Belyanskaya, P. Manser, P. Spohn, A. Bruinink and P. Wick, The reliability and limits of the MTT reduction assay for carbon nanotubes–cell interaction, *Carbon*, 2007, **45**, 2643–2648.
31 B. R. Coleman, T. Knight, V. Gies, Z. J. Jakubek and S. Zou, Manipulation and quantification of graphene oxide flake size: Photoluminescence and cytotoxicity, *ACS Appl. Mater. Interfaces*, 2017, **9**, 28911–28921.
32 S. K. Sohaebuddin, P. T. Thevenot, D. Baker, J. W. Eaton and L. Tang, Nanomaterial cytotoxicity is composition, size, and cell type dependent, *Part. Fibre Toxicol.*, 2010, **7**, 22.
33 J. Farkas and A. M. Booth, Are fluorescence-based chlorophyll quantification methods suitable for algae toxicity assessment of carbon nanomaterials?, *Nanotoxicology*, 2017, **11**, 569–577.
34 M. Wu, R. Kempaiah, P.-J. J. Huang, V. Maheshwari and J. Liu, Adsorption and desorption of DNA on graphene oxide studied by fluorescently labeled oligonucleotides, *Langmuir*, 2011, **27**, 2731–2738.
35 K. P. Loh, Q. Bao, G. Eda and M. Chhowalla, Graphene oxide as a chemically tunable platform for optical applications, *Nat. Chem.*, 2010, **2**, 1015–1024.
36 L. Zha, J. Hu, C. Wang, S. Fu and M. Luo, The effect of electrolyte on the colloidal properties of poly (N-isopropylacrylamide-co-dimethylaminoethylmethacrylate) microgel latexes, *Colloid Polym. Sci.*, 2002, **280**, 1116–1121.
37 D. J. Stephens and V. J. Allan, Light microscopy techniques for live cell imaging, *Science*, 2003, **300**, 82–86.
38 T. L. Riss, R. A. Moravec, A. L. Niles, S. Duellman, H. A. Benink, T. J. Worzella and L. Minor, *Cell viability assays. In Assay Guidance Manual*, Eli Lilly & Company and the National Center for Advancing Translational Sciences, Bethesda (MD), USA, 2016.
39 M. Ginouves, B. Carme, P. Couppie and G. Prevot, Comparison of tetrazolium salt assays for evaluation of drug activity against Leishmania spp, *J. Clin. Microbiol.*, 2014, **52**, 2131–2138.
40 F. Joris, B. B. Manshian, K. Peynshaert, S. C. De Smedt, K. Braeckmans and S. J. Soenen, Assessing nanoparticle toxicity in cell-based assays: Influence of cell culture parameters and optimized models for bridging the in vitro–in vivo gap, *Chem. Soc. Rev.*, 2013, **42**, 8339–8359.
41 M. Pavlin and V. B. Bregar, Stability of nanoparticle suspensions in different biologically relevant media, *Dig. J. Nanomater. Bio.*, 2012, **7**, 1389–1400.
42 O. Akhavan and E. Ghaderi, Toxicity of graphene and graphene oxide nanowalls against bacteria, *ACS Nano*, 2010, **4**, 5731–5736.